

First-principles study of the stability of the icosahedral Ti_{13} , Ti_{13}^{-1} , and Ti_{13}^{+1} clusters

Shan-Ying Wang,¹ Wenhui Duan,¹ Dong-Liang Zhao,² and Chong-Yu Wang^{1,2}

¹*Department of Physics, Tsinghua University, Beijing 100084, China*

²*Center Iron and Steel Research Institute, Beijing 100081, China*

(Received 7 June 2001; revised manuscript received 20 August 2001; published 10 April 2002)

DMol cluster method based on density-functional theory has been used to study the structural stability of icosahedral Ti_{13} , Ti_{13}^{-1} , and Ti_{13}^{+1} clusters. The calculated results show that Ti_{13} , Ti_{13}^{-1} , and Ti_{13}^{+1} clusters favor a D_{3d} structure due to Jahn-Teller effect. However, for neutral Ti_{13} and positively charged Ti_{13}^{+1} clusters, the binding energies of the I_h and D_{5d} structures are quite close to that of the D_{3d} structure. The small distortion from the icosahedron in the D_{3d} structure is consistent with the prediction from the collision-induced dissociation experiment on positively charged Ti_{13}^{+1} cluster. The structural distortion in the charged clusters and the bonding feature in the neutral icosahedral Ti_{13} cluster are discussed. In addition, all the clusters in the present study are found to be magnetic and show small magnetic moments.

DOI: 10.1103/PhysRevB.65.165424

PACS number(s): 36.40.Cg, 36.40.Qv, 31.15.Ar

I. INTRODUCTION

In the past two decades, transition-metal (TM) clusters, due to their unique physical and chemical properties, have attracted much attention in scientific and technological fields. In comparison with the cluster composed of sp metal atoms, TM clusters have enormous complexity and do not exhibit the electronic shell effects due to the unfilled d shell. Most of their properties are dominated by the localized behavior of d electrons. Although without the striking shell effects, TM clusters with some specific number (i.e., magic number) of atoms exhibit the pronounced characteristics in experimental spectra, and show high structural stability and other interesting properties, which makes them promising in the synthesis of nanostructure system.

The structural stability and the electronic structure are two important coupled questions in the cluster research, and the knowledge on them can give us more insight into the physical and chemical properties of clusters. However, the geometrical structure and the electronic structure of TM cluster could not be easily determined by experiments, because there are often several low-lying structural isomers whose energies are very close to that of the ground state. Many techniques such as mass-spectrum and photoelectron spectroscopy have been applied to the cluster research, yielding much valuable, but usually indirect or incomplete information. While combined with the experimental approach, the first-principles method based on density-functional theory^{1,2} (DFT) and the method based on semiempirical potential^{3,4} are proved to be effective in the cluster research, particularly in predicting the geometrical structure.

TM cluster systems composed of $3d$ elements Fe, Ni, and Co have been intensively studied.⁵⁻¹² By use of density-functional theory, Castro, Jamorski, and Salahub systematically investigated structure, bonding, and magnetism of small Fe, Ni, and Co clusters.⁹⁻¹² They fully demonstrated the effect of Jahn-Teller distortion and the effect of cluster size on the structural, electronic, and magnetic properties. On the other hand, people still have limited knowledge on the cluster systems composed of the fore part of $3d$ elements such as V, Ti, and Cr, even these systems might be less

complicated in geometrical structure, electronic structure, and magnetism. In the cluster research, the icosahedral structure is often regarded as one of the most interesting structures. The collision-induced dissociation experiment¹³ on the positive Ti clusters suggested that Ti_{13}^{+1} cluster prefer icosahedral packing. In order to clarify the stable structure for the neutral and the charged Ti_{13} clusters, we have performed energy gradient and total-energy calculations on the neutral and charged Ti_{13} clusters with different symmetry by use of first-principles method. In this paper, we report our study on the structural stability of icosahedral Ti_{13} , Ti_{13}^{-1} , and Ti_{13}^{+1} clusters.

II. THEORETICAL METHOD

First-principles DMol method^{14,15} based on DFT have been employed in the present study. In DMol method, the energy gradient for each atom can be conveniently calculated, and the equilibrium atomic structure and the total energy of the ground state can be obtained by relaxing the atoms until the forces acting on the atoms become zero.

As well known, the basis set and the exchange-correlation functional used in the localized-orbital method could affect the calculated results to some extent. DMol method provides a variety of forms for the basis set and the exchange-correlation functional. The double-numerical basis with polarized functions was proved to be the best choice for basis set. For TM atom, the inner orbitals such as $3s$ and $3p$ sometimes play an essential role in determining the ground-state properties. This is particularly true for ultrafine Ti clusters.¹⁶

Due to the insufficiency in describing the strong correlation effect of the localized d electron, local-density approximation (LDA) sometimes yields inaccurate bond length and total energy for TM cluster. The general gradient approximation (GGA) correction may be a better choice.¹² First of all, using several kinds of exchange-correlation functionals, we have performed all-electron test calculations on Ti_2 dimer. The functionals used in the test are denoted as BLYP, BPW, PW, and LDA. The first two (BLYP and BPW) are constructed by combining the correlation functional of either Lee, Yang, and Par¹⁷ (LYP) or Perdew and Wang¹⁸ (PW)

TABLE I. Calculated atomic bond lengths a_0 (in Å) and binding energies E_b (in eV) of Ti_2 dimer at the ground state.

	BLYP	BPW	PW	LDA	Expt.
a_0	1.974	1.961	1.958	1.902	1.9429 ± 0.0013^a
E_b	-3.999	-4.354	-4.504	-5.105	-1.349^b

^aResonant two-photon ionization: Ref. 28.

^bLower bound from resonant two-photon ionization: Ref. 29.

with exchange functional of Becke¹⁹ (B). The third (PW) is constructed on the basis of the exchange and the correlation functionals of Perdew and Wang.¹⁸ The last one (LDA) utilizes the scheme proposed by Vosko, Wilk, and Nusair.²⁰ The results of test calculations are summarized in Table I. Obviously, the results of GGA are much closer to the experimental data than those of LDA. The errors of BPW functional lie between those of BLYP functional and those of PW functional.

In a recent study on Ti_2 dimer, Barden, Rienstra-Kiracafe, and Schaefer²¹ found that the pure DFT functionals BLYP and the correlation functional proposed by Perdew in 1986 (Refs. 22,23) are the best choices. In consideration of our above calculated results and the work by Barden, Rienstra-Kiracafe, and Schaefer,²¹ we adopted the double-numerical basis with polarized functions and the exchange-correlation functional of BPW in the present study, and performed all-electron spin-unrestricted calculations. The convergence criteria of optimization were 0.0001 eV Å^{-1} and 0.0001 Å for energy gradient and atomic displacement, respectively. The charge density was converged to 1×10^{-8} , which corresponds to a total-energy convergence of $1 \times 10^{-6} \text{ eV}$. The maximum angular momentum of the multipolar fitting function was chosen to be one greater than the maximum angular momentum in the atomic-orbital basis, and about 1500 fixed integration points were used for each atom.

III. RESULT AND DISCUSSION

In order to reveal the stability of neutral and charged icosahedral Ti_{13} clusters, we performed DMol optimization calculations on Ti_{13} , Ti_{13}^{-1} , and Ti_{13}^{+1} clusters with I_h , D_{3d} , D_{5d} , and D_{2h} symmetry, respectively. The sketch of the geometrical structure of the cluster system is shown in Fig. 1. The calculated results are summarized in Tables II and III. The binding energy of the cluster system is defined as the difference in the total energy between the interacting atom system and the free-atom system.

From Table II, we can see that for Ti_{13} , Ti_{13}^{-1} , and Ti_{13}^{+1} clusters, the configuration with the D_{3d} symmetry has the lowest energy, and the configuration with the D_{2h} symmetry has the highest energy that is about 0.10 to 0.30 eV higher than that of other configurations, suggesting that the D_{2h} structure is unstable. We should also point out that for neutral Ti_{13} and positively charged Ti_{13}^{+1} clusters, the energies of the I_h and D_{5d} structures are quite close to that of the D_{3d} structure, with a difference as small as several or tens of meV. Aware of the level of the present exchange-correlation functionals, we would like to regard the D_{3d} , I_h , and D_{5d} struc-

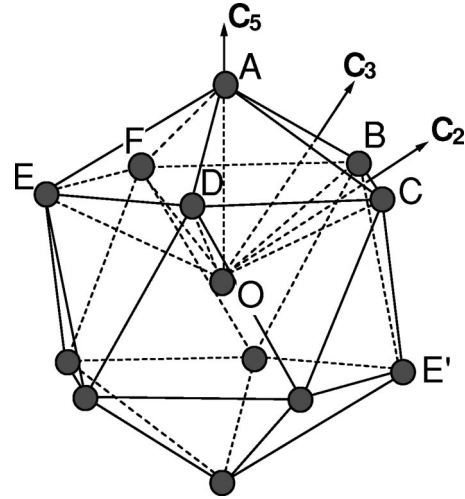


FIG. 1. Structural sketch of Ti_{13} cluster. The atoms are symbolized by solid balls. Some atoms are labeled by letters O, A, B, C, D, E, F, and E' for the convenience of discussion. C_5 , C_3 , and C_2 denote the main axes in the clusters with the D_{5d} , D_{3d} , and D_{2h} symmetries, respectively.

tures as degenerate isomers for neutral Ti_{13} and positively charged Ti_{13}^{+1} clusters. To our knowledge, the experimental and theoretical studies on neutral and charged Ti clusters are rather scarce. Using a guided ion-beam mass spectrometer, Lian, Su, and Armentrout¹³ studied collision-induced dissociation of Ti_n^+ ($n=2\sim 22$), and suggested that Ti_{13}^{+1} cluster favors icosahedral structures. From Table III, we can see that the distortions from the icosahedron in the D_{3d} and D_{5d} structures are quite small. Such small distortions of the icosahedron are consistent with the prediction of Lian, Su, and Armentrout.¹³ We find that from the positive cluster to the negative cluster, the difference in the binding energy between D_{3d} and D_{5d} structures increases but that between D_{5d} and I_h (I_h and D_{2h}) structures decreases. This implies that the extra one electron could enhance the atomic bonding in D_{3d} structure, and thus is in favor of stabilizing the D_{3d} structure.

The results of the binding energy reflect the complexity of TM cluster: there are many low-lying states with very close energies. From Jahn-Teller theorem,²⁴ we know that an electronic system occupying an energy level with degeneracy is unstable against a structural distortion that removes that degeneracy in first order. In other words, the system can be stabilized by a structural distortion that removes the degeneracy of levels. The Jahn-Teller effect exists in the cluster systems of high symmetry, especially in the systems whose highest-occupied molecular orbital (HOMO) is of high degeneracy and is not fully occupied. For Ti_{13} , Ti_{13}^{-1} , and Ti_{13}^{+1} clusters with the I_h structure, the HOMO is the triplet state T_{1u} of spin-down. The calculated results of energies confirm the presence of Jahn-Teller effect in Ti_{13} , Ti_{13}^{-1} , and Ti_{13}^{+1} clusters, i.e., the distortion from I_h structure to D_{3d} structure. While from Table II, we can see that the degeneracy is not fully removed in the neutral D_{3d} structure, which still has the unfilled HOMO, a twofold degenerate state E_u of spin-down. As mentioned by Alonso,²⁵ there are two factors that deter-

TABLE II. Calculated binding energy E_b (in eV), the HOMO state, the energy difference ΔE between the LUMO and HOMO, the electron occupation number n in the HOMO, the total spin S , the atomic magnetic moment M (in μ_B), and the atomic charge Q in Ti_{13} , Ti_{13}^{-1} , and Ti_{13}^{+1} clusters with different symmetry. The symbols I_h , I_h^{-1} and I_h^{+1} denote Ti_{13} , Ti_{13}^{-1} , and Ti_{13}^{+1} cluster with the I_h symmetry respectively, and other symbols in the first column are defined in a similar way. The symbols “+” and “-” in the third column denote spin-up and spin-down state, respectively. The letters O, A, B, and D denote the atomic sites shown in Fig. 1.

Sym.	E_b	HOMO	ΔE	n	S	M				Q			
						O	A	B	D	O	A	B	D
I_h	-54.2010	$T_{1u}(-)$	0.146	2	3	0.202	0.483	0.483	0.483	-0.617	0.051	0.051	0.051
I_h^{-1}	-55.5089	$T_{1u}(-)$	0.054	3	2.5	0.126	0.406	0.406	0.406	-0.372	-0.052	-0.052	-0.052
I_h^{+1}	-49.6419	$T_{1u}(-)$	0.220	1	3.5	0.283	0.560	0.560	0.560	-0.813	0.151	0.151	0.151
D_{3d}	-54.2242	$E_u(-)$	0.100	1	3	0.201	0.455	0.455	0.511	-0.575	0.052	0.052	0.044
D_{3d}^{-1}	-55.6453	$A_{1g}(+)$	0.138	1	2.5	0.067	0.384	0.384	0.438	-0.520	-0.029	-0.029	-0.051
D_{3d}^{+1}	-49.7054	$A_{2g}(-)$	0.053	1	3.5	0.279	0.496	0.496	0.624	-0.782	0.154	0.154	0.143
D_{5d}	-54.2192	$E_{1u}(-)$	0.099	1	3	0.201	0.403	0.499	0.499	-0.625	0.053	0.052	0.052
D_{5d}^{-1}	-55.5154	$A_{2u}(-)$	0.049	1	2.5	0.127	0.392	0.409	0.409	-0.367	-0.054	-0.053	-0.053
D_{5d}^{+1}	-49.7043	$E_{2g}(+)$	0.069	2	3.5	0.271	0.458	0.581	0.581	-0.828	0.162	0.150	0.150
D_{2h}	-54.0424	$B_{2g}(-)$	0.078	1	2	0.087	0.214	0.423	0.341	-0.839	0.043	0.094	0.073
D_{2h}^{-1}	-55.4393	$A_g(-)$	0.103	1	1.5	0.017	0.078	0.220	0.447	-0.716	-0.062	-0.040	0.030
D_{2h}^{+1}	-49.4148	$A_g(+)$	0.085	1	1.5	0.052	0.075	0.377	0.285	-0.930	0.144	0.155	0.184

mine the most possible equilibrium geometry of TM cluster. One is that the compact structure has the maximum number of bonds, and the other is that the directional bonding is compatible with the orientation and the filling of d orbitals. The latter factor appears to promote the occurrence of Jahn-Teller effect. The two factors, both beneficial in enhancing the binding energy, are disadvantageous to each other. Therefore, the equilibrium structure depends on the competition between the two factors. Obviously, the filling of $3d$ orbitals plays a dominative role in determining the equilibrium structure of Ti_{13} , Ti_{13}^{-1} , and Ti_{13}^{+1} clusters.

Now we discuss the effects of extra charge on atomic bond length. Table III presents the calculated bond lengths

for some bonds in Ti_{13} , Ti_{13}^{-1} , and Ti_{13}^{+1} clusters. We can classify the bonds (refer to Fig. 1) as the perpendicular, the parallel, and the tilted bonds according to their orientation relative to the main axis of the group. The characteristic perpendicular bonds for the I_h , D_{3d} , D_{5d} , and D_{2h} structures are {BC}, {AB}, {BC}, and {OD, BC} respectively; the characteristic parallel bonds for the I_h , D_{5d} , and D_{2h} structures are {OA}, {OA}, and {AE}, respectively; and the characteristic tilted bonds for the I_h , D_{3d} , D_{5d} , and D_{2h} structures are {OB, AB}, {OA, OD, AD, AE, DE}, {OB, AB}, and {OA, OB, AB, AD, CD}, respectively. For the I_h structure, it can be found that the extra one electron in the negatively charged cluster almost has no effect on the bond length, but the bond

TABLE III. Calculated bond lengths (in Å) in Ti_{13} , Ti_{13}^{-1} , and Ti_{13}^{+1} clusters with different symmetry. The symbols I_h , I_h^{-1} , and I_h^{+1} denote the I_h structures of Ti_{13} , Ti_{13}^{-1} , and Ti_{13}^{+1} cluster, respectively, and other symbols in the first column are defined in a similar way. The letters O, A, B, and D denote the atomic sites shown in Fig. 1.

Sym.	OA		OB, OC		OD, OF		OE		AB, AC		AD, AF		AE		BC		CD, FB		DE, EF	
I_h	2.567	2.567	2.567	2.567	2.567	2.567	2.699	2.699	2.699	2.699	2.699	2.699	2.699	2.699	2.699	2.699	2.699	2.699	2.699	2.699
I_h^{-1}	2.567	2.567	2.567	2.567	2.567	2.567	2.699	2.699	2.699	2.699	2.699	2.699	2.699	2.699	2.699	2.699	2.699	2.699	2.699	2.699
I_h^{+1}	2.576	2.576	2.576	2.576	2.576	2.576	2.708	2.708	2.708	2.708	2.708	2.708	2.708	2.708	2.708	2.708	2.708	2.708	2.708	2.708
D_{3d}	2.580	2.580	2.556	2.556	2.556	2.556	2.692	2.694	2.725	2.692	2.694	2.725	2.692	2.694	2.694	2.695	2.695	2.695	2.695	2.695
D_{3d}^{-1}	2.531	2.531	2.604	2.604	2.604	2.604	2.713	2.634	2.738	2.713	2.634	2.738	2.713	2.634	2.634	2.785	2.785	2.785	2.785	2.785
D_{3d}^{+1}	2.604	2.604	2.550	2.550	2.550	2.550	2.685	2.708	2.757	2.685	2.708	2.757	2.685	2.708	2.708	2.690	2.690	2.690	2.690	2.690
D_{5d}	2.586	2.564	2.564	2.564	2.564	2.564	2.693	2.693	2.693	2.687	2.687	2.687	2.687	2.687	2.687	2.687	2.687	2.687	2.687	2.687
D_{5d}^{-1}	2.562	2.569	2.569	2.569	2.569	2.569	2.696	2.696	2.696	2.700	2.700	2.700	2.700	2.700	2.700	2.700	2.700	2.700	2.700	2.700
D_{5d}^{+1}	2.644	2.563	2.563	2.563	2.563	2.563	2.708	2.708	2.708	2.676	2.676	2.676	2.676	2.676	2.676	2.676	2.676	2.676	2.676	2.676
D_{2h}	2.648	2.562	2.484	2.648	2.648	2.648	2.717	2.631	2.803	2.591	2.722	2.631	2.591	2.722	2.631	2.631	2.631	2.631	2.631	2.631
D_{2h}^{-1}	2.632	2.585	2.480	2.632	2.632	2.632	2.714	2.601	2.777	2.551	2.762	2.601	2.551	2.762	2.601	2.601	2.601	2.601	2.601	2.601
D_{2h}^{+1}	2.647	2.586	2.500	2.647	2.647	2.647	2.716	2.596	2.852	2.667	2.744	2.596	2.667	2.744	2.596	2.596	2.596	2.596	2.596	2.596

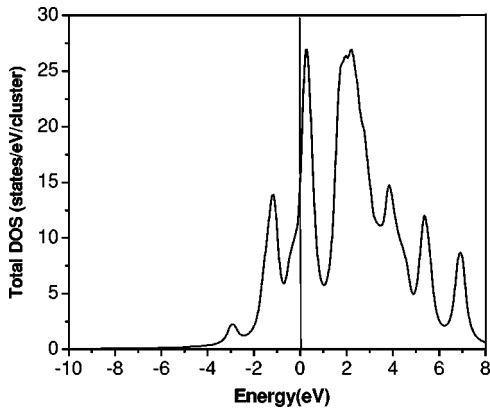


FIG. 2. TDOS of the neutral icosahedral Ti_{13} cluster. The Fermi level is shifted to zero.

lengths in the positively charged cluster increases comparing with that in the neutral cluster. For the D_{3d} and D_{5d} structures, there are two remarkable types of distortion in the charged clusters comparing to the neutral cluster: the perpendicular and the parallel distortions with respect to the main axis. For example, in the negative D_{3d} structure, we can see that the bond length of AB increases but the bond length of OA decreases, which means the expansion of the equilateral triangle ABC perpendicular to the C_3 axis and the inward movement along the C_3 axis toward the center (i.e., point O in Fig. 1). Furthermore, the enlarged bond lengths of OD and DE as well as the reduced bond length of AD in the negative D_{3d} structure reveal the expansion of another larger equilateral triangle FDE' perpendicular to the C_3 axis and the outward movement along the C_3 axis. These distortions can enhance the tilted bonds such as AD and OA, and weaken the perpendicular bonds such as AB in the negative D_{3d} structure. We can see that the distortions in the positive D_{3d} structure are exactly opposite to those in the negative D_{3d} structure, and obviously, the way of the variation of bond lengths in the D_{5d} structure is similar to the case in the D_{3d} structure. For the charged D_{2h} structure, the bond lengths of the perpendicular bond BC and the parallel bond AE show remarkable variations with respect to those in the neutral D_{2h} structure, and these variations in the negative D_{2h} structure are opposite to those in the positive D_{2h} structure either. The above results clarify the effect of extra charge on the atomic structure of Ti_{13} cluster: the gain of one electron could make the structure longitudinally contracted but transversely expanded, and the effect of the loss of one electron is just the reverse of the gain of one electron.

Figure 2 presents the calculated total density of states (TDOS) of the neutral Ti_{13} cluster with the I_h symmetry. The TDOS curve displays several noticeable peaks, which are mainly composed of the hybrid states of s , p , and d electrons. This can be clearly seen from the partial density-of-states (PDOS) curves shown in Figs. 3 and 4. The small peak appearing at about -3.0 eV implies the hybrid states of $4s$ of central Ti atom with $3p$ and $4s$ of apex Ti atoms. The two peaks that lie separately just above and below the Fermi level reveal that the hybrid states are composed of all valence orbitals in the cluster, and these strong hybrid states domi-

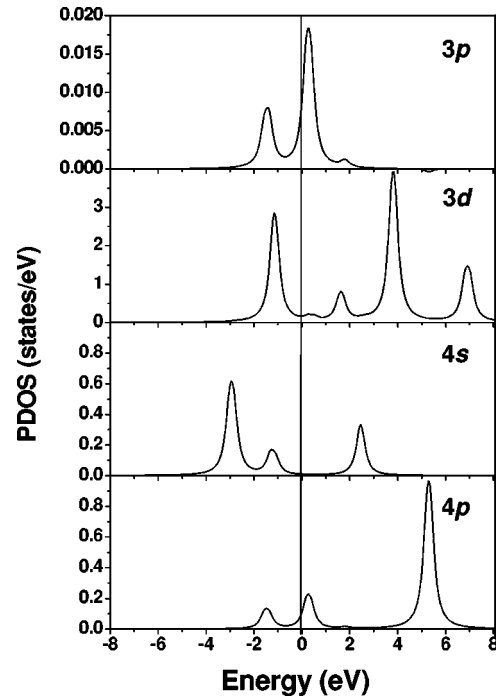


FIG. 3. PDOS of the central Ti atom in the neutral icosahedral Ti_{13} cluster. The Fermi level is shifted to zero.

nate the bonding characteristic in the cluster. We can see that the states in the energy range from 1.0 to 8.0 eV include mainly the strong s , p , and d hybrid states of apex Ti atoms, and some hybrid states of atomic orbitals of central Ti atom with those of apex Ti atoms. Since there are fewer $3d$ electrons in Ti, the bonding feature in the neutral icosahedral Ti_{13}

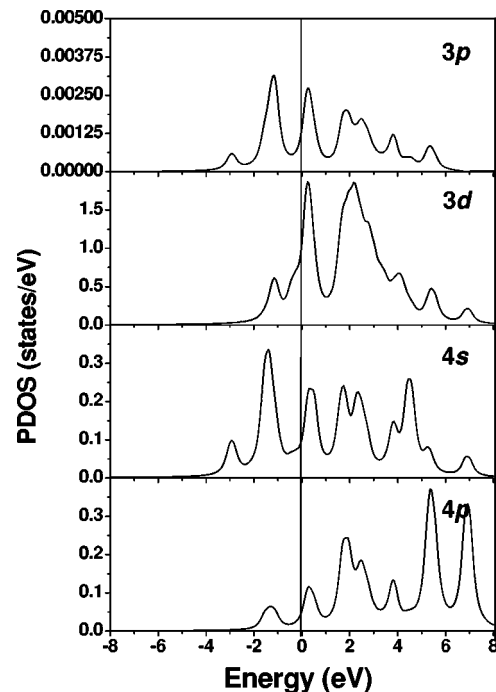


FIG. 4. PDOS of apex Ti atom in the neutral icosahedral Ti_{13} cluster. The Fermi level is shifted to zero.

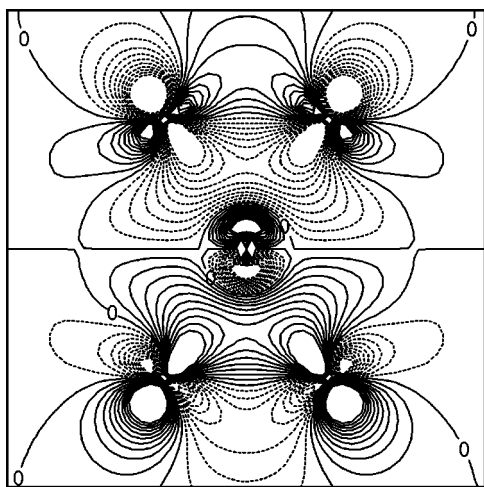


FIG. 5. Contour of one of the HOMO's in the neutral icosahedral Ti_{13} cluster.

cluster is somewhat different from that in other icosahedral $3d$ TM clusters such as Co_{13} and Ni_{13} .^{6,8} Here, the $s, p-d$ hybridizations is more important and the role of s electron increases. All the states below the Fermi level are the bonding states. As an illustration, we give in Fig. 5 the contour plot of one of the HOMO's in the neutral icosahedral Ti_{13} cluster. The contour curves clearly show the interaction between $4p$ of central Ti atom and $3d$ of apex Ti atoms. We can find that the bonding feature in the Ti_{13} cluster is very close to that in the hexagonal bulk Ti obtained by energy-band calculation,²⁶ which indicates the emergence of bulk feature in the Ti_{13} cluster. This agrees with the result of photoelectron spectroscopy experiment.²⁷ However, we must notice that the characteristic bond lengths in the icosahedral Ti_{13} cluster still are much shorter than the bond length (2.95 Å) of the hexagonal bulk Ti metal.

From the data in Table II, we can find that all clusters considered are magnetic and exhibit small magnetic moments. For all structures, the gain of one electron will result in a 0.5 decrease of the total spin of the cluster. The loss of one electron still has the effect opposite to that caused by the gain of one electron: it will result in a 0.5 increase of the

total spin of cluster, with exception of the D_{2h} structure. The magnetic moment of the central Ti atom is smaller than that of the apex Ti atom. This is similar to the case in Co_{13} and Ni_{13} clusters,^{6,8} where the magnetic moment of central atom significantly reduces due to the presence of the apex atoms. The phenomenon can be understood simply from the filling of $3d$ orbitals. The large coordination number of the central Ti atom results in the enhancement of the overlap of its $3d$ orbitals with those of other apex Ti atoms, which can reduce the exchange splitting of its $3d$ orbitals and consequently weaken its magnetism. The charge transfers from the apex Ti atom to the central Ti atom in the neutral or positively charged cluster, and the central Ti atom can gain even more electrons in the negatively charged cluster. Some of these gained electrons occupy the $3d$ spin-down states, which reduce the magnetic moment of central Ti atom.

IV. SUMMARY

We have studied the structural stability of icosahedral Ti_{13} , Ti_{13}^{-1} , and Ti_{13}^{+1} clusters by use of DMol method based on density-functional theory. Our results show that Ti_{13} , Ti_{13}^{-1} , and Ti_{13}^{+1} clusters favors a D_{3d} structure through Jahn-Teller distortion. However, for neutral Ti_{13} and positively charged Ti_{13}^{+1} clusters, the energies of the I_h and D_{5d} structures are quite close to that of the D_{3d} structure. The small distortion from the icosahedron in the D_{3d} structure is consistent with the prediction from the collision-induced dissociation experiment on positively charged Ti_{13}^{+1} cluster. The structural distortions caused by the gain of one electron and the loss of one electron are opposite to each other, and both consist of the longitudinal and the transverse distortions with respect to the main axis. The $s, p-d$ hybridizations are important in the neutral icosahedral cluster. All the clusters are found to be magnetic and exhibit small magnetic moments.

ACKNOWLEDGMENTS

This research was supported by the "973" Project from the Ministry of Science and Technology of China (Grant No. G2000067102) and Chinese Natural Science Foundation (Grant Nos. 10104010 and 59801009).

¹P. C. Hohenberg and W. Kohn, Phys. Rev. **136**, B864 (1964).

²W. Kohn and L. J. Sham, Phys. Rev. **140**, A1133 (1965).

³M. Menon, J. Connolly, N. N. Lathiotakis, and A. N. Andriotis, Phys. Rev. B **50**, 8903 (1994).

⁴N. N. Lathiotakis, A. N. Andriotis, M. Menon, and J. Connolly, J. Chem. Phys. **104**, 992 (1996).

⁵P. Ballone and R. O. Jones, Chem. Phys. Lett. **233**, 632 (1995).

⁶Z. Q. Li and B. L. Gu, Phys. Rev. B **47**, 13 611 (1993).

⁷F. A. Reuse and S. N. Khanna, Chem. Phys. Lett. **234**, 77 (1995).

⁸F. A. Reuse, S. N. Khanna, and S. Bernerl, Phys. Rev. B **52**, R11 650 (1995).

⁹M. Castro, Int. J. Quantum Chem. **64**, 223 (1997).

¹⁰M. Castro, C. Jamorski, and D. R. Salahub, Chem. Phys. Lett.

271, 133 (1997).

¹¹G. A. Cisneros, M. Castro, and D. R. Salahub, Int. J. Quantum Chem. **75**, 847 (1999).

¹²M. Pereiro, D. Baldomir, M. Iglesias, C. Rosales, and M. Castro, Int. J. Quantum Chem. **81**, 422 (2001).

¹³L. Lian, C.-X. Su, and P. B. Armentrout, J. Chem. Phys. **97**, 4084 (1992).

¹⁴B. Delley, J. Chem. Phys. **92**, 508 (1990).

¹⁵B. Delley, J. Chem. Phys. **94**, 7245 (1991).

¹⁶S. H. Wei, Z. Zeng, J. Q. You, X. H. Yan, and X. G. Gong, J. Chem. Phys. **113**, 11 127 (2000).

¹⁷C. Lee, W. Yang, and R. G. Parr, Phys. Rev. B **37**, 785 (1988).

¹⁸J. P. Perdew and Y. Wang, Phys. Rev. B **45**, 13 244 (1992).

- ¹⁹A. D. Becke, Phys. Rev. A **38**, 3098 (1988).
- ²⁰S. J. Vosko, L. Wilk, and M. Nusair, Can. J. Phys. **58**, 1200 (1980).
- ²¹C. J. Barden, J. C. Rienstra-Kiracofe, and H. F. Schaefer III, J. Chem. Phys. **113**, 690 (2000).
- ²²J. P. Perdew, Phys. Rev. B **33**, 8822 (1986).
- ²³J. P. Perdew, Phys. Rev. B **34**, 7406 (1986).
- ²⁴H. A. Jahn and E. Teller, Proc. R. Soc. London, Ser. A **161**, 220 (1937).
- ²⁵J. A. Alonso, Chem. Rev. **100**, 637 (2000).
- ²⁶O. Jepsen, Phys. Rev. B **12**, 2988 (1975).
- ²⁷H. B. Wu, S. R. Desai, and L. S. Wang, Phys. Rev. Lett. **76**, 212 (1996).
- ²⁸M. Doverstal, L. Karlsson, B. Lindgren, and U. Sassenberg, Chem. Phys. Lett. **270**, 273 (1997).
- ²⁹M. Doverstal, B. Lindgren, U. Sassenberg, C. A. Arrington, and M. D. Morse, J. Chem. Phys. **97**, 7087 (1992).